

Strings in the Extended BTZ Spacetime

Samuli Hemming¹, Esko Keski-Vakkuri¹, and Per Kraus²

¹*Helsinki Institute of Physics,*

P.O. Box 64, FIN-00014 University of Helsinki, Finland

`samuli.hemming@helsinki.fi`, `esko.keski-vakkuri@helsinki.fi`

²*Department of Physics and Astronomy*

UCLA, Los Angeles, CA 90095-1547, U.S.A.

`pkraus@physics.ucla.edu`

We study string theory on the extended spacetime of the BTZ black hole, as described by an orbifold of the $SL(2, \mathbb{R})$ WZW model. The full spacetime has an infinite number of disconnected boundary components, each corresponding to a dual CFT. We discuss the computation of bulk and boundary correlation functions for operators inserted on different components. String theory correlation functions are obtained by analytic continuation from an orbifold of the $SL(2, \mathbb{C})/SU(2)$ coset model. This yields two-point functions for general operators, including those describing strings that wind around the horizon of the black hole.

1. Introduction

The BTZ black hole spacetime [1] possesses many features that one would like to understand better in string theory: event horizons, Hawking radiation, time dependence, nontrivial causal structure with potential closed timelike curves, etc. Since the corresponding worldsheet theory is an orbifold of the $SL(2,\mathbb{R})$ WZW model, classical string theory is in principle exactly solvable in this background. Furthermore, being asymptotically AdS_3 , the theory has a dual holographic description as a $1+1$ dimensional CFT. For all these reasons, it seems fruitful to gain a detailed understanding of string theory in the BTZ spacetime.

Early work concerning strings on BTZ includes [2,3,4,5]. However, progress was delayed by an incomplete understanding of the underlying $SL(2,\mathbb{R})$ WZW model: an *ad hoc* cutoff on the spectrum seemed to be needed for unitarity. It is now known [6] that instead of imposing a cutoff one should include long strings and spectral flowed states in the spectrum (see also [7,8]), and that the resulting theory is unitary. In light of this new understanding, [9] elaborated on the earlier work [4] on the string spectrum in BTZ and interpreted it in the context of spectral flow. Additional related work can be found in [10,11,12,13,14]. Here we would like to continue this program, focussing on the string theory interpretation of the extended BTZ geometry, and evaluating some simple correlation functions in this background.

The maximal extension of the rotating BTZ black hole has an intricate causal structure with multiple asymptotic regions, analogous to the Kerr solution in asymptotically flat spacetime. The multiple boundaries of the spacetime lead to a richer example of holography than usual, with the possibility of computing correlation functions of operators inserted on disconnected boundary components. This is similar to what one can expect for certain cosmological spacetimes, with distinct boundaries in the far past and future; for recent examples see [15,16,17]. We would like to know the rules for relating bulk and boundary correlation functions in such a situation.¹

Given a spacetime with spacelike separated disconnected boundaries, it is known that the Hilbert space of the dual CFT is the product of the CFT Hilbert spaces corresponding to the distinct boundary components [18,19,20,21]. In the case of a black hole, tracing over an unobserved Hilbert space yields a thermal density matrix for the remaining space. As discussed in [21] this can be understood by analytic continuation from the Euclidean black hole; for example wavefunctions in the left and right halves of the Kruskal diagram for a nonrotating black hole are related by the imaginary time evolution $t \rightarrow t + i\beta/2$, yielding a Boltzmann factor. In the case of string theory, analytic continuation from

¹ The physical relevance of the extended spacetime can be questioned due to potentially destabilizing backreaction effects; we discuss this more in the text.

Euclidean signature takes on added significance, since we do not at present know how to compute correlation functions directly in Lorentzian signature. As we discuss, correlations among non-spacelike separated boundary components can also be found by continuation from Euclidean signature, and the result can again be related to correlation functions in a tensor product Hilbert space. This gives a holographic interpretation of the extended BTZ solution.

String theory correlation functions in AdS_3 were obtained in [22] by analytically continuing results from the $\text{SL}(2,\mathbb{C})/\text{SU}(2)$ model [23]. We can apply the same strategy in the BTZ case, starting from the appropriate orbifold of the $\text{SL}(2,\mathbb{C})/\text{SU}(2)$ model. The main difference is that one needs to work in the hyperbolic basis for the current algebra, rather than the elliptic basis normally used for AdS_3 . In this basis, the spectral flow operation of [6] generates strings that wind around the black hole horizon [9]. We will focus on the two point functions for vertex operators of flowed and unflowed string states. Ultimately, one would like to describe interaction in this background, including loop effects, in order to see what string theory has to say about the BTZ singularity.

The remainder of this paper is organized as follows. In section 2 we review the geometry of the extended BTZ spacetime, in particular the structure of the boundary, and the relations between the different coordinate patches. Section 3 discusses correlation functions in the field theory limit. We review some relevant aspects of AdS_3 string theory in section 4. String theory correlation functions in BTZ are computed in section 5, and in section 6 we conclude with a discussion of some open problems. In an attempt to make this paper approximately self-contained we have included a substantial amount of review material. A reader who is very familiar with the extended BTZ geometry can safely skim much of section 2, and similarly section 4 for the reader well versed in AdS_3 string theory.

2. Causal structure of the BTZ black hole

We begin by reviewing the extended BTZ geometry, paying special attention to the structure of the boundary. The BTZ geometry is of course well understood from the original work [1]. In those papers it was proposed to truncate the geometry at a “singularity” in order to avoid the presence of closed timelike curves. Ultimately, this can only be justified by doing calculations in the full quantum theory, since closed timelike curves can be consistent at the classical level. Here our focus is on classical string physics and so we will keep the full spacetime including the regions with closed timelike curves.

2.1. Lorentzian black hole

The BTZ black hole is obtained by making identifications in AdS_3 . AdS_3 is defined by the hyperboloid

$$x_0^2 + x_1^2 - x_2^2 - x_3^2 = \ell^2. \tag{2.1}$$

This is also the $SL(2, \mathbb{R})$ group manifold,

$$g = \frac{1}{\ell} \begin{pmatrix} x_1 + x_2 & x_3 + x_0 \\ x_3 - x_0 & x_1 - x_2 \end{pmatrix}, \quad \det g = 1. \quad (2.2)$$

Henceforth, we will always consider the covering space of the group manifold, sometimes denoted as $CAdS_3$. The AdS_3 metric is the invariant metric on the group manifold,

$$ds^2 = -\ell^2 \text{Tr} g^{-1} dg g^{-1} dg. \quad (2.3)$$

The isometry group of AdS_3 is therefore $SL(2, \mathbb{R})_L \times SL(2, \mathbb{R})_R$, acting as

$$g \rightarrow g_L g g_R. \quad (2.4)$$

$SL(2, \mathbb{R})$ has three types of conjugacy classes:

$$\begin{aligned} \text{hyperbolic : } & |\text{Tr } g| > 2, \quad g = h \begin{pmatrix} \alpha & 0 \\ 0 & \alpha^{-1} \end{pmatrix} h^{-1}, \\ \text{elliptic : } & |\text{Tr } g| < 2, \quad g = h \begin{pmatrix} \cos \alpha & \sin \alpha \\ -\sin \alpha & \cos \alpha \end{pmatrix} h^{-1}, \\ \text{parabolic : } & |\text{Tr } g| = 2, \quad g = \pm h \begin{pmatrix} 1 & 1 \\ 0 & 1 \end{pmatrix} h^{-1}. \end{aligned} \quad (2.5)$$

To define the BTZ black hole we identify by elements of a hyperbolic conjugacy class

$$g \cong \rho_L g \rho_R, \quad (2.6)$$

with

$$\rho_L = \begin{pmatrix} e^{2\pi^2 T_+} & 0 \\ 0 & e^{-2\pi^2 T_+} \end{pmatrix}, \quad (2.7)$$

$$\rho_R = \begin{pmatrix} e^{2\pi^2 T_-} & 0 \\ 0 & e^{-2\pi^2 T_-} \end{pmatrix},$$

and $T_+ \leq T_-$. The radii of the inner and outer horizons of the black hole, r_- and r_+ , are related to T_{\pm} by

$$\begin{aligned} r_+ &= \pi \ell (T_+ + T_-), \\ r_- &= -\pi \ell (T_+ - T_-). \end{aligned} \quad (2.8)$$

The mass and angular momentum of the black hole are

$$\begin{aligned} M &= 2\pi^2 (T_+^2 + T_-^2) = \frac{r_+^2 + r_-^2}{\ell^2} \\ J &= -2\pi^2 \ell (T_+^2 - T_-^2) = \frac{2r_+ r_-}{\ell}. \end{aligned} \quad (2.9)$$

The identifications (2.7) act as a boost in the $x_1 - x_2$ and $x_0 - x_3$ planes:

$$\begin{pmatrix} x_1 \\ x_2 \\ x_3 \\ x_0 \end{pmatrix} \cong \begin{pmatrix} \cosh \gamma_+ & \sinh \gamma_+ & 0 & 0 \\ \sinh \gamma_+ & \cosh \gamma_+ & 0 & 0 \\ 0 & 0 & \cosh \gamma_- & -\sinh \gamma_- \\ 0 & 0 & -\sinh \gamma_- & \cosh \gamma_- \end{pmatrix} \begin{pmatrix} x_1 \\ x_2 \\ x_3 \\ x_0 \end{pmatrix}, \quad \gamma_{\pm} = \frac{2\pi r_{\pm}}{\ell}. \quad (2.10)$$

The identification has no fixed points in the rotating case with $r_- \neq 0$. In the non-rotating case $r_- = 0$ there are fixed points at $x_1 = x_2 = 0$. This line of fixed points is what BTZ call the singularity of the non-rotating BTZ black hole.

The identification (2.10) gives rise to closed timelike curves. In the non-rotating case this is easily seen by examining the geometry in the neighborhood of the fixed points,

$$\begin{aligned} x_1 &= \mathcal{O}(\epsilon), \\ x_2 &= \mathcal{O}(\epsilon), \\ x_3 &= \pm \sqrt{-\ell^2 + x_0^2} + \mathcal{O}(\epsilon^2) \end{aligned} \quad (2.11)$$

giving the metric

$$ds^2 = -dx_1^2 + dx_2^2 + \frac{dx_0^2}{1 - x_0^2/\ell^2} + \mathcal{O}(\epsilon^2). \quad (2.12)$$

So near the fixed point the identification (2.10) acts as a boost in $R^{1,1}$, which is a timelike identification for $|x_2| > |x_1|$. In the rotating case the identification (2.10) also shifts x_0 , thereby smoothing out the orbifold.

To get a picture of the global structure we divide the original AdS_3 manifold into the following 3 types of regions

$$\begin{aligned} \text{Region 1 : } & x_1^2 - x_2^2 \geq 0, \quad x_0^2 - x_3^2 \leq 0, \\ \text{Region 2 : } & x_1^2 - x_2^2 \geq 0, \quad x_0^2 - x_3^2 \geq 0, \\ \text{Region 3 : } & x_1^2 - x_2^2 \leq 0, \quad x_0^2 - x_3^2 \geq 0. \end{aligned} \quad (2.13)$$

The original AdS_3 manifold is best thought of as a solid cylinder with an $S^1 \times R$ boundary. Which regions reach the boundary? The AdS_3 boundary is given by taking (this will become more apparent when we introduce explicit coordinates)

$$\begin{aligned} |x_1^2 - x_2^2| &\rightarrow \infty \\ |x_0^2 - x_3^2| &\rightarrow \infty, \end{aligned} \quad (2.14)$$

subject of course to (2.1). From (2.13) and (2.14) it is apparent that region 2 does not extend out to the boundary, while regions 1 and 3 do. Regions 1 and 2 are both bounded by an asymptotic boundary at infinity and an event horizon. So from the perspective of

either region 1 or 3 the other two regions lie behind the horizon. As we'll review, region 3 contains closed timelike curves, and the “singularity” of the BTZ black hole is located at the boundary of the ergosphere ($g_{tt} = 0$ in stationary coordinates) of region 3.

The geometry is easier to visualise in the non-rotating case, so we consider this first. The boundaries separating adjacent regions define null hypersurfaces in AdS_3 ; drawing these in the AdS_3 cylinder we obtain figure 1.

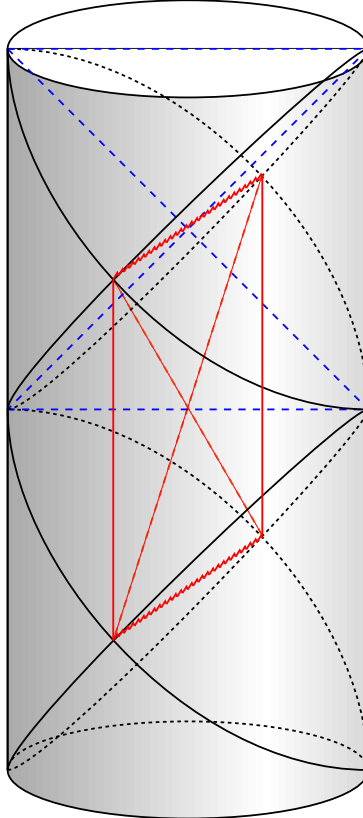


Fig. 1: The AdS_3 cylinder. Depicted in the figure are the null hypersurfaces separating regions 2 and 3, as well as two colored vertical cross sections yielding Penrose diagrams. The standard Penrose diagram appears as the red square, also displayed in figure 2. The perpendicular blue square gives the Penrose diagram of figure 3.

Penrose diagrams are obtained by drawing two dimensional vertical cross sections of the cylinder, as in figures 2 and 3.

The Penrose diagram in figure 2 is the standard one with the singularity appearing as a spacelike hypersurface, and the region 3 containing the closed timelike curves does not appear. In figure 1, which depicts the AdS cylinder, the standard diagram appears as

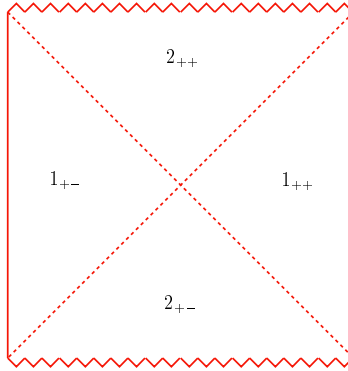


Fig. 2: The standard non-rotating BTZ Penrose diagram.

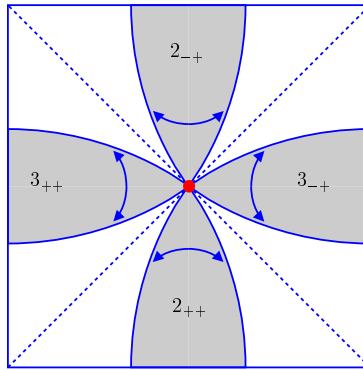


Fig. 3: The Penrose diagram showing region 3, with identifications indicated

1

the rectangle in the center². The perpendicular vertical cross section of the cylinder³ gives the Penrose diagram of figure 3. In the latter Penrose diagram region 3 is displayed while region 1 is absent. See [13] for some other depictions of the geometry.

We now introduce explicit coordinates for the general rotating black hole. The BTZ identifications will preserve two Killing vectors out of the original six, and we take u_+ and u_- to be coordinates labelling the orbits of these Killing vectors, as well as the radial coordinate r . This requires that we cover each of the regions 1,2,3 by four separate coordinate patches. We henceforth work in units where $\ell = 1$. In the following $\eta_{1,2} = \pm 1$.

² Shown in red if colors are displayed.

³ Shown in blue.

1

Region 1:

$$\begin{aligned}
x_1 &= \eta_1 \left(\frac{r^2 - r_-^2}{r_+^2 - r_-^2} \right)^{1/2} \cosh \pi(T_+ u_+ + T_- u_-) \\
x_2 &= \eta_1 \left(\frac{r^2 - r_-^2}{r_+^2 - r_-^2} \right)^{1/2} \sinh \pi(T_+ u_+ + T_- u_-) \\
x_3 &= \eta_2 \left(\frac{r^2 - r_+^2}{r_+^2 - r_-^2} \right)^{1/2} \cosh \pi(T_+ u_+ - T_- u_-) \\
x_0 &= \eta_2 \left(\frac{r^2 - r_+^2}{r_+^2 - r_-^2} \right)^{1/2} \sinh \pi(T_+ u_+ - T_- u_-).
\end{aligned} \tag{2.15}$$

Region 2:

$$\begin{aligned}
x_1 &= \eta_1 \left(\frac{r^2 - r_-^2}{r_+^2 - r_-^2} \right)^{1/2} \cosh \pi(T_+ u_+ + T_- u_-) \\
x_2 &= \eta_1 \left(\frac{r^2 - r_-^2}{r_+^2 - r_-^2} \right)^{1/2} \sinh \pi(T_+ u_+ + T_- u_-) \\
x_3 &= \eta_2 \left(\frac{r_+^2 - r^2}{r_+^2 - r_-^2} \right)^{1/2} \sinh \pi(T_+ u_+ - T_- u_-) \\
x_0 &= \eta_2 \left(\frac{r_+^2 - r^2}{r_+^2 - r_-^2} \right)^{1/2} \cosh \pi(T_+ u_+ - T_- u_-).
\end{aligned} \tag{2.16}$$

Region 3:

$$\begin{aligned}
x_1 &= \eta_1 \left(\frac{r^2 - r_+^2}{r_+^2 - r_-^2} \right)^{1/2} \sinh \pi(T_+ u_+ - T_- u_-) \\
x_2 &= \eta_1 \left(\frac{r^2 - r_+^2}{r_+^2 - r_-^2} \right)^{1/2} \cosh \pi(T_+ u_+ - T_- u_-) \\
x_3 &= \eta_2 \left(\frac{r^2 - r_-^2}{r_+^2 - r_-^2} \right)^{1/2} \sinh \pi(T_+ u_+ + T_- u_-) \\
x_0 &= \eta_2 \left(\frac{r^2 - r_-^2}{r_+^2 - r_-^2} \right)^{1/2} \cosh \pi(T_+ u_+ + T_- u_-).
\end{aligned} \tag{2.17}$$

In all three regions u_{\pm} range over all real values. $r_+ \leq r \leq \infty$ in regions 1 and 3; $r_- \leq r \leq r_+$ in region 2.

We define t and ϕ by

$$u_{\pm} = \phi \pm t. \tag{2.18}$$

The BTZ identification (2.6) in these coordinates is

$$\begin{aligned}
\text{Regions 1, 2: } & (t, \phi, r) \cong (t, \phi + 2\pi, r) \\
\text{Region 3: } & (t, \phi, r) \cong (t + 2\pi, \phi, r).
\end{aligned} \tag{2.19}$$

The solution written in t, ϕ, r coordinates is

$$ds^2 = -\frac{(r^2 - r_+^2)(r^2 - r_-^2)}{r^2} dt^2 + \frac{r^2}{(r^2 - r_+^2)(r^2 - r_-^2)} dr^2 + r^2 \left(d\phi - \frac{r_+ r_-}{r^2} dt \right)^2. \quad (2.20)$$

In string theory we also have a nonvanishing NS-NS B-field. In these coordinates it is

$$B = \begin{cases} (r^2 - r_-^2) d\phi \wedge dt & \text{regions 1, 2} \\ (r^2 - r_+^2) d\phi \wedge dt & \text{region 3.} \end{cases} \quad (2.21)$$

More precisely, we have twelve patches corresponding to regions 1,2,3 and four choices for $\eta_{1,2}$. The full spacetime consists of an infinite vertical stack of these patches. The Penrose diagram of the rotating black hole is obtained from (2.20). Dropping the third term in (2.20), writing the remainder as $ds^2 = \Omega^2(x^+, x^-) dx^+ dx^-$, and assembling the different patches, we arrive at figure 4. This figure indicates the causal structure in the $t - r$ plane. However, note that null geodesics will not remain in this plane; this in contrast to the Penrose diagram for the four dimensional Kerr solution, which is drawn along the axis of symmetry of the black hole.

We chose our coordinates so that the metric takes the same form in all three regions and so that t is a timelike coordinate for large r , but note that this implies that r jumps when we cross from region 2 to 3. In particular, the boundary between regions 2 and 3 is at $r = r_-$ when viewed from region 2, and $r = r_+$ when viewed from region 3. For the same reason the B-field changes form in (2.21), though the change is just a gauge transformation.

From (2.20) it is clear that the BTZ identification is spacelike in regions 1 and 2, and timelike in region 3 for $r > (r_-^2 + r_+^2)^{1/2}$. What is referred to as the singularity of the rotating BTZ solution is the boundary of the ergosphere, $r = (r_-^2 + r_+^2)^{1/2}$ in region 3. If the geometry is truncated here then there will be no closed timelike curves.

For computing correlation functions in the extended BTZ geometry it is very useful to note that we can use analytic continuation to go from one region to another. For instance, starting in region 1_{++} (meaning $\eta_1 = \eta_2 = +1$) we can continue to the other three regions $1_{\eta_1 \eta_2}$ by making the replacements

$$\begin{aligned} 1_{+-} : \quad T_{\pm} u_{\pm} &\rightarrow T_{\pm} u_{\pm} \mp \frac{i}{2} \\ 1_{-+} : \quad T_{\pm} u_{\pm} &\rightarrow T_{\pm} u_{\pm} - \frac{i}{2} \\ 1_{--} : \quad T_{+} u_{+} &\rightarrow T_{+} u_{+} - i \\ &u_{-} \rightarrow u_{-}. \end{aligned} \quad (2.22)$$

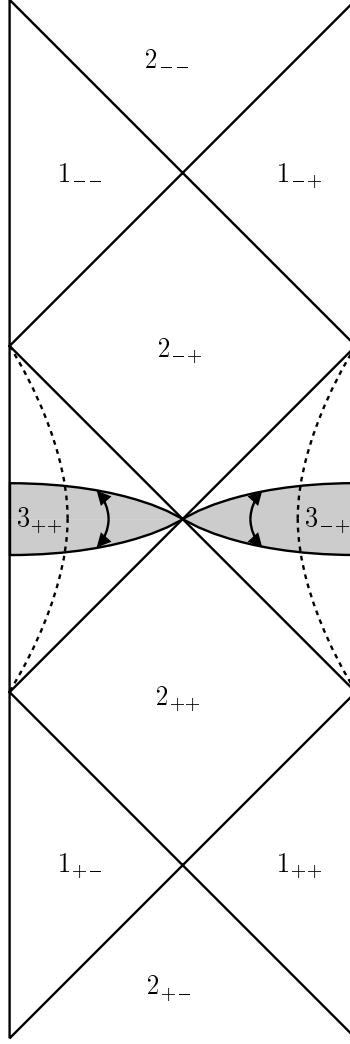


Fig. 4: The Penrose diagram of the rotating BTZ black hole. Dashed lines represent what BTZ called the singularity. Arrows indicate the identifications, which become timelike when extended past the singularity.

Similarly, to go from region $1_{\eta_1\eta_2}$ to region $3_{\eta_1\eta_2}$ we take

$$\begin{aligned}
 T_+ u_+ &\rightarrow T_+ u_+ - \frac{i}{2} \\
 u_- &\rightarrow -u_- \\
 r^2 &\rightarrow r_+^2 + r_-^2 - r^2.
 \end{aligned}
 \tag{2.23}$$

We chose the signs of the imaginary parts for later convenience; flipping these just takes one to another copy of the respective region.

2.2. Boundary structure

Regions 1 and 3 have boundaries at $r \rightarrow \infty$. The metric on the boundary is

$$ds^2 = r^2(-dt^2 + d\phi^2) \quad (2.24)$$

with the identifications (2.19). In both cases the boundary is an infinite cylinder, with the circle direction being spacelike in region 1 and timelike in region 3.

It is helpful to study how the boundary of the original AdS₃ cylinder is broken up by the identifications. Global coordinates for AdS₃ are

$$\begin{aligned} x_1 &= \cosh \mu \cos \tau \\ x_2 &= \sinh \mu \sin \theta \\ x_3 &= \sinh \mu \cos \theta \\ x_0 &= \cosh \mu \sin \tau, \end{aligned} \quad (2.25)$$

with metric

$$ds^2 = -\cosh^2 \mu d\tau^2 + d\mu^2 + \sinh^2 \mu d\theta^2. \quad (2.26)$$

Consider the boundary region, $\mu \rightarrow \infty$. The boundary is conformal to the cylinder $ds^2 = -d\tau^2 + d\theta^2$, with $\theta \cong \theta + 2\pi$. At the boundary the coordinate transformation between global and BTZ coordinates becomes

Region 1:

$$\tan \frac{\tau \pm \theta}{2} = (\pm \tanh \pi T_{\pm} u_{\pm})^{\eta_1 \eta_2} \quad (2.27)$$

Region 3:

$$\tan \frac{\tau \pm \theta}{2} = (\pm \tanh \pi T_{\pm} u_{\pm})^{-\eta_1 \eta_2}. \quad (2.28)$$

The original boundary in global coordinates therefore breaks up into eight separate patches, repeated with periodicity $\Delta\tau = 2\pi$; see Figure 5.

The BTZ identifications on the boundary are inherited from (2.19):

$$\begin{aligned} \text{Regions 1, 2: } & (t, \phi) \cong (t, \phi + 2\pi) \\ \text{Region 3: } & (t, \phi) \cong (t + 2\pi, \phi). \end{aligned} \quad (2.29)$$

For holography, it is important to identify the topology of the boundary. From Figure 5 it appears that the boundaries of regions 1 and 3 touch one another, but this is misleading. From the definitions (2.13) it is clear that it is impossible to go from region 1 to region 3, or vice versa, without passing through region 2. On the other hand, region 2 does not extend out to the boundary, since r is bounded as $r_- \leq r \leq r_+$. Therefore, the BTZ boundary is disconnected. As we will discuss in more detail later, according to

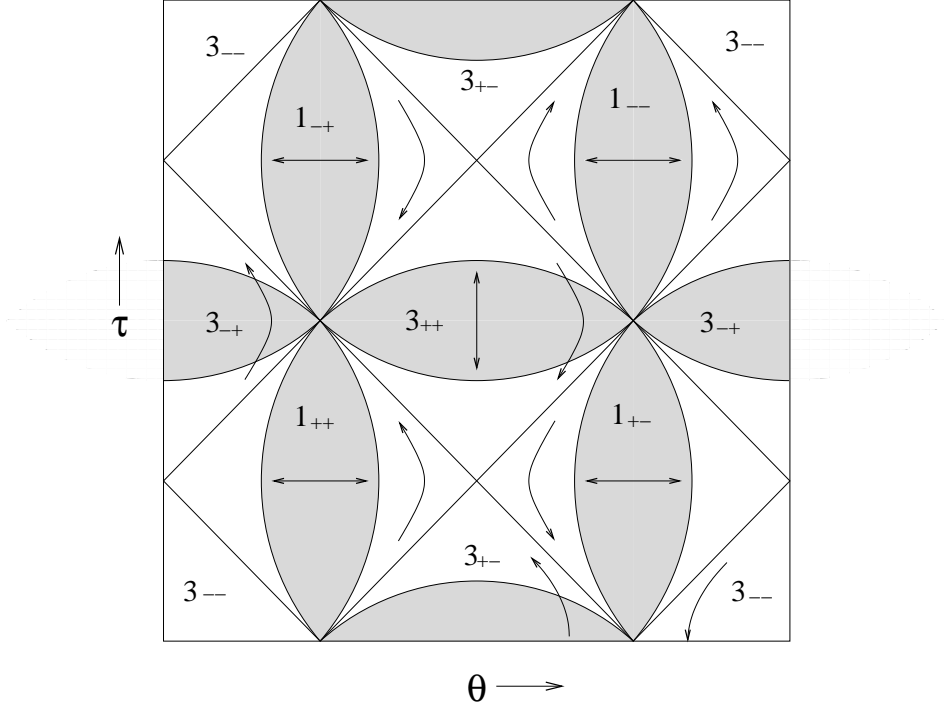


Fig. 5: The boundary. Shaded areas are fundamental domains under the identifications. Lines with double arrows indicate the identifications. Lines with single arrows indicate the flow of time.

the AdS/CFT correspondence the bulk theory is then dual to a CFT living on the full disconnected boundary. The main question which needs to be addressed is how to relate bulk correlation functions to correlation functions of the CFT living on this disconnected space. We will answer this momentarily, but the point to be emphasized now is that since the BTZ and AdS₃ spacetimes have a different boundary structure they correspond to distinct boundary theories; the BTZ solution should *not* be thought of as a particular state in the CFT corresponding to AdS₃. This is in contrast to a collapse geometry in which a black hole forms in the bulk; in that case the boundary is a single connected cylinder, and we expect to be able to describe the black hole by a pure state in the corresponding CFT.

2.3. Euclidean black hole

Computing string theory correlation functions directly in the Lorentzian signature BTZ spacetime is challenging since the worldsheet action is unbounded from below. In such situations one proceeds by analytically continuing to Euclidean signature, computing correlation functions there, and then continuing back. This strategy was employed for pure AdS₃ in [22] and we wish to do the same for BTZ.

To continue we take $t \rightarrow i\tau$, or equivalently

$$u_+ \rightarrow u = \phi + i\tau, \quad u_- \rightarrow \bar{u} = \phi - i\tau, \quad (2.30)$$

where \bar{u} denotes complex conjugate. The metric (2.20) then becomes complex. To obtain a real metric we take r_- pure imaginary, or equivalently

$$T_+ \rightarrow T, \quad T_- \rightarrow \bar{T}. \quad (2.31)$$

The metric becomes

$$ds^2 = \frac{(r^2 - r_+^2)(r^2 - r_-^2)}{r^2} d\tau^2 + \frac{r^2}{(r^2 - r_+^2)(r^2 - r_-^2)} dr^2 + r^2 \left(d\phi - \frac{r_+(ir_-)}{r^2} d\tau \right)^2. \quad (2.32)$$

The radial coordinate has the range $r_+ \leq r \leq \infty$. The identifications are now

$$(u, r) \cong (u + 2\pi, r) \cong (u + i\beta, r), \quad (2.33)$$

where the complex Euclidean inverse temperature is $\beta = \frac{1}{T}$. The boundary of the Euclidean black hole is therefore a torus with modular parameter $i\beta/(2\pi)$.

3. Supergravity correlation functions

We now turn to the computation of correlation functions in the extended BTZ geometry. As compared to the usual AdS/CFT setup the novelty here is the disconnected boundary and the presence of horizons and closed timelike curves. We want to establish the rules for computing correlation functions in the bulk and boundary, as well as the relation between them. As usual, it is simplest to start by restricting attention to the low energy field theory in the bulk; the full string theory is considered in section 5. In this section we always work in Lorentzian signature.

The simplest correlators are one-point functions, in particular the expectation value of the boundary energy momentum tensor. On each boundary this is given by [24]

$$T_{\mu\nu} = \frac{1}{8\pi G} (\Theta_{\mu\nu} - \Theta\gamma_{\mu\nu} - \gamma_{\mu\nu}) \quad (3.1)$$

where $\gamma_{\mu\nu}$ is the boundary metric and $\Theta_{\mu\nu}$ is its extrinsic curvature. Since the metric takes the form (2.20) in all regions, the energy momentum tensor is the same on all boundaries:

$$\begin{aligned} T_{tt} = T_{\phi\phi} &= \frac{M}{2\pi} \\ T_{t\phi} = T_{\phi t} &= \frac{J}{2\pi}, \end{aligned} \quad (3.2)$$

with the mass and angular momentum given in (2.9). In region 1 ϕ has 2π periodicity, so integrating $T_{\mu\nu}$ over ϕ gives the total energy and angular momentum M and J . On the other hand, in region 3 ϕ is noncompact, so the constant $T_{\mu\nu}$ leads to an infinite total energy and angular momentum.

Now consider two-point functions corresponding to minimally coupled bulk scalars of mass m . As usual, the two-point functions follow directly from the bulk-boundary propagator [25,26]. It is convenient to start with the expression for the AdS₃ bulk-boundary propagator written in Poincaré coordinates with line element,

$$ds^2 = \frac{dy^2 + dw_+ dw_-}{y^2}. \quad (3.3)$$

The bulk-boundary propagator behaves near the $y = 0$ boundary as $y^{2h_-} \delta^{(2)}(\Delta w_+, \Delta w_-)$, with $\Delta w_{\pm} = w_{\pm} - w'_{\pm}$, and corresponds to a boundary operator of mass dimension $2h_+$, where

$$h_{\pm} = \frac{1}{2}(1 \pm \sqrt{1 + m^2}). \quad (3.4)$$

The bulk-boundary propagator is then

$$K_{\text{AdS}_3}(y, w_+, w_-; w'_+, w'_-) = c \left(\frac{y}{y^2 + \Delta w_+ \Delta w_-} \right)^{2h_+}. \quad (3.5)$$

This can be rewritten in BTZ coordinates for region 1_{++} using the transformation:

$$\begin{aligned} w_{\pm} &= \sqrt{\frac{r^2 - r_+^2}{r^2 - r_-^2}} e^{2\pi T_{\pm} u_{\pm}} \\ y &= \sqrt{\frac{r_+^2 - r_-^2}{r^2 - r_-^2}} e^{\pi(T_+ u_+ + T_- u_-)}. \end{aligned} \quad (3.6)$$

The resulting expression has boundary behavior $e^{-2\pi h_+(T_+ u'_+ + T_- u'_-)} r^{-2h_-} \delta^{(2)}(\Delta u_+, \Delta u_-)$, so we should further multiply by $e^{2\pi h_+(T_+ u'_+ + T_- u'_-)}$ to get the correct BTZ propagator. Finally, we should impose periodicity under the BTZ identifications by including a sum over images. We first assume that both arguments of the propagator are in region 1_{++} , and denote this by $K_{\text{BTZ}}^{(1_{++}1_{++})}$. To evaluate two point functions we only need the result for large r , which is

$$\begin{aligned} &K_{\text{BTZ}}^{(1_{++}1_{++})}(r, u_+, u_-; u'_+, u'_-) \\ &= c' \sum_{n=-\infty}^{\infty} \frac{\left(\frac{r_+^2 - r_-^2}{r^2}\right)^{h_+} e^{-2\pi h_+[T_+ \Delta u_+ + T_- \Delta u_- + (T_+ + T_-)2\pi n]}}{\left\{ \frac{r_+^2 - r_-^2}{r^2} + (1 - e^{-2\pi T_+ (\Delta u_+ + 2\pi n)})(1 - e^{-2\pi T_- (\Delta u_- + 2\pi n)}) \right\}^{2h_+}}. \end{aligned} \quad (3.7)$$

Following the standard procedure gives the two-point function [27]

$$\begin{aligned} & \langle \mathcal{O}_{1_{++}}(u_+, u_-) \mathcal{O}_{1_{++}}(u'_+, u'_-) \rangle \\ & \sim \sum_{n=-\infty}^{\infty} [\sinh \pi T_+(\Delta u_+ + 2\pi n)]^{-2h_+} [\sinh \pi T_-(\Delta u_- + 2\pi n)]^{-2h_+}. \end{aligned} \quad (3.8)$$

Before considering the two-point functions for operators inserted on other boundaries, we should note that the bulk-boundary propagator (3.7) is not the only possible choice. As always in Lorentzian versions of the AdS/CFT correspondence [28], it is possible to add a solution of the bulk wave equation with boundary behavior r^{-2h_+} . (3.7) is a natural propagator to take as it is the one which arises upon analytic continuation from Euclidean signature. This corresponds to evaluating expectation values in a particular state of the dual CFT; other choices for the propagator correspond to considering other states.

To find two-point functions on other boundaries we can use the analytic continuation given in (2.22) and (2.23). In particular, fixing u'_\pm to be on a fixed boundary, we can use (2.22) to compute the propagator on the full extended BTZ spacetime and then read off the resulting correlation functions. As above, using analytic continuation implicitly commits one to considering a particular state of the CFT defined on the full disconnected BTZ boundary. We will discuss more below whether the analytic continuation is justified.

There are eight possible choices for inserting each of the two operators, $1_{\pm\pm}$ and $3_{\pm\pm}$ (actually there are an infinite number of copies of each, but given the overall periodicity these do not need to be discussed separately). Since only Δu_\pm appears in (3.8) it is clear that the same two point function is obtained whenever both operators are inserted on the same boundary. Now consider operators on distinct boundaries. Without loss of generality we can take u'_\pm on boundary 1_{++} . Continuing u_\pm to the other boundaries then gives

$$\begin{aligned} & \langle \mathcal{O}_{\eta_1 \eta_2}(u_+, u_-) \mathcal{O}_{1_{++}}(u'_+, u'_-) \rangle = \\ & 1_{++} : \sum_{n=-\infty}^{\infty} [\sinh \pi T_+(\Delta u_+ + 2\pi n)]^{-2h_+} [\sinh \pi T_-(\Delta u_- + 2\pi n)]^{-2h_+} \\ & 1_{+-} : \sum_{n=-\infty}^{\infty} [\cosh \pi T_+(\Delta u_+ + 2\pi n)]^{-2h_+} [\cosh \pi T_-(\Delta u_- + 2\pi n)]^{-2h_+} \\ & 1_{-+} : \sum_{n=-\infty}^{\infty} [\cosh \pi T_+(\Delta u_+ + 2\pi n)]^{-2h_+} [\cosh \pi T_-(\Delta u_- + 2\pi n)]^{-2h_+} \\ & 1_{--} : \sum_{n=-\infty}^{\infty} [\sinh \pi T_+(\Delta u_+ + 2\pi n)]^{-2h_+} [\sinh \pi T_-(\Delta u_- + 2\pi n)]^{-2h_+} \end{aligned} \quad (3.9)$$

and similarly continuing to boundaries of the regions 3:

$$\begin{aligned}
& \langle \mathcal{O}_{\eta_1 \eta_2}(u_+, u_-) \mathcal{O}_{1_{++}}(u'_+, u'_-) \rangle = \\
& 3_{++} : \sum_{n=-\infty}^{\infty} [\cosh \pi T_+(\Delta u_+ + 2\pi n)]^{-2h_+} [\sinh \pi T_-(u_- + u'_- - 2\pi n)]^{-2h_+} \\
& 3_{+-} : \sum_{n=-\infty}^{\infty} [\sinh \pi T_+(\Delta u_+ + 2\pi n)]^{-2h_+} [\cosh \pi T_-(u_- + u'_- - 2\pi n)]^{-2h_+} \\
& 3_{-+} : \sum_{n=-\infty}^{\infty} [\sinh \pi T_+(\Delta u_+ + 2\pi n)]^{-2h_+} [\cosh \pi T_-(u_- + u'_- - 2\pi n)]^{-2h_+} \\
& 3_{--} : \sum_{n=-\infty}^{\infty} [\cosh \pi T_+(\Delta u_+ + 2\pi n)]^{-2h_+} [\sinh \pi T_-(u_- + u'_- - 2\pi n)]^{-2h_+}.
\end{aligned} \tag{3.10}$$

These two-point functions are periodic under

$$(t, \phi) \rightarrow (t + i\beta_H, \phi + i\Omega\beta_H), \tag{3.11}$$

where β_H is the inverse Hawking temperature and Ω is the angular velocity of the outer horizon,

$$\begin{aligned}
\beta_H &= \frac{1}{T_H} = \frac{T_+ + T_-}{2T_+T_-} \\
\Omega &= -\frac{T_+ - T_-}{T_+ + T_-}.
\end{aligned} \tag{3.12}$$

3.1. Boundary description of correlators

In the boundary description a CFT is defined on each component of the boundary. We should be able to relate the above bulk correlators to correlators in this collection of CFTs. Since the CFTs are defined on distinct surfaces, they will only communicate with each other via correlations in their initial conditions and by boundary conditions. These can be deduced from the analytic continuations taking us from one region to another. For operators inserted in regions 1_{++} and 1_{+-} this was discussed in detail in [21].

Consider inserting an operator \mathcal{O} in a given region, say 1_{++} . We then perform the CFT path integral over this region with boundary conditions at $t = \pm\infty$ labelled by wavefunctionals $\Psi_{1_{++}}(t = \pm\infty)$, yielding

$$\langle \Psi'_{1_{++}}(t = \infty) | \mathcal{O}_{1_{++}} | \Psi_{1_{++}}(t = -\infty) \rangle. \tag{3.13}$$

We can do the same on another boundary, say 1_{+-} . Since the analytic continuation (2.22) is $(t, \phi) \rightarrow (t - i\beta_H/2, \phi - i\Omega\beta_H/2)$ the states in the two regions are related by

$$|\Psi_{1_{+-}}(t = \pm\infty)\rangle = \langle \Psi_{1_{++}}(t = \pm\infty) | e^{-\beta_H(H - \Omega J)/2}, \tag{3.14}$$

where the change from ket to bra occurs because time runs in opposite directions in the two regions. We will suppress the normalization factors in state vectors. Therefore, the path integral in the two regions summed over all boundary conditions gives (up to normalization):

$$\sum_{E,E',J,J'} e^{-\beta_H(E+E'-\Omega J-\Omega J')/2} \langle E, J | \mathcal{O}_{1_{+-}} | E', J' \rangle \langle E', J' | \mathcal{O}_{1_{++}} | E, J \rangle. \quad (3.15)$$

This result can be interpreted as follows. First rewrite states and operators in 1_{+-} in terms of their time reversed versions, so that time runs in the same direction in both regions. Recall that time reversal acts as $\langle T\chi | T\psi \rangle = \langle \psi | \chi \rangle$. Then consider the tensor product of the two Hilbert spaces, and the particular correlated state

$$|\Psi\rangle = \sum_{E,J} e^{-\beta_H(E-\Omega J)/2} |E, J\rangle_{1_{+-}} |E, J\rangle_{1_{++}}. \quad (3.16)$$

We find that (3.15) is equivalent to the expectation value in this state:

$$\langle \Psi | \mathcal{O}_{1_{+-}} \mathcal{O}_{1_{++}} | \Psi \rangle. \quad (3.17)$$

If we do not insert any operator in 1_{+-} then we recover a thermal expectation value for $\mathcal{O}_{1_{++}}$:

$$\langle \mathcal{O}_{1_{++}} \rangle_{\beta_H, \Omega} = \sum_{E,J} e^{-\beta_H(E-\Omega J)} \langle E, J | \mathcal{O}_{1_{++}} | E, J \rangle. \quad (3.18)$$

This structure is very natural from the bulk point of view. Regions 1_{++} and 1_{+-} are spacelike separated and so operators in distinct regions commute. Furthermore, one needs to combine spacelike hypersurfaces in both regions in order to get a complete spacelike hypersurface for the full spacetime. Therefore, the full Hilbert space is described by a tensor product of the two Hilbert spaces, and the precise correlation in (3.16) corresponds to considering a black hole in thermal equilibrium. All of this then carries over to the boundary theory.

Insertions of operators in 1_{-+} and 1_{--} are interpreted similarly. To continue from 1_{++} to 1_{-+} we take $(t, \phi) \rightarrow (t - i\Omega\beta_H/2, \phi - i\beta_H/2)$, therefore the path integral is

$$\sum_{E,E',J,J'} e^{-\beta_H(\Omega E + \Omega E' - J - J')/2} \langle E, J | \mathcal{O}_{1_{-+}} | E', J' \rangle \langle E', J' | \mathcal{O}_{1_{++}} | E, J \rangle, \quad (3.19)$$

which corresponds to an expectation value in the correlated state

$$|\Psi\rangle = \sum_{E,J} e^{-\beta_H(\Omega E - J)/2} |E, J\rangle_{1_{-+}} |E, J\rangle_{1_{++}}. \quad (3.20)$$

Region 1_{--} corresponds to the state (in this case no time reversal is required)

$$|\Psi\rangle = \sum_{E,J} e^{-(1+\Omega)\beta_H(E-J)/2} |E, J\rangle_{1_{--}} |E, J\rangle_{1_{++}}. \quad (3.21)$$

Actually, there is a fundamental difference in the three cases we have considered in that region 1_{+-} is spacelike separated in the bulk from 1_{++} , while 1_{-+} and 1_{--} lie to the future of 1_{++} . Since in the last two cases we are computing correlation functions for operators inserted in causally connected regions, it may seem unnatural to be introducing a tensor product Hilbert space. In the latter cases, the tensor product Hilbert space does not correspond to the space of physical states of the theory, but is better thought of as a device for computing correlation functions. According to the AdS/CFT correspondence we should be able to relate all bulk observables to quantities in the boundary theory, and to do this it turns out to be useful to employ the product Hilbert space description. On the other hand, from the bulk spacetime geometry it is clear that it *is* sensible to combine regions 1_{-+} and 1_{--} into a tensor product, since one thereby obtains a family of spacelike hypersurfaces. These hypersurfaces lie to the future of those corresponding to region 1_{++} and 1_{+-} , and so the respective states are related by Hamiltonian evolution.

Now consider inserting an operator in region 3. The CFT in each boundary component of region 3 lives on a cylinder with the compact direction being timelike, as compared to region 1 where the compact direction is spacelike. We will only consider region 3_{++} to avoid undue repetition. The continuation from region 1_{++} is $(t, \phi) \rightarrow (\phi - i(1+\Omega)\beta_H/2, t - i(1+\Omega)\beta_H/2)$. The continuation maps the wavefunctions defined at early and late times in 1_{++} to wavefunctions defined at spacelike infinity in 3_{++} . Therefore, E and J eigenvalues are interchanged, which is expected since E should have an integer spectrum in region 3_{++} due to the timelike identification there. Following the same logic as before, we then find that correlators can be reproduced by taking expectation values in the state

$$|\Psi\rangle = \sum_{E,J} e^{-(1+\Omega)\beta_H(E-J)/2} |J, E\rangle_{3_{++}} |E, J\rangle_{1_{++}}. \quad (3.22)$$

We now ask whether the expectation value of operators in the states we have defined yield the two-point functions in (3.9) (3.10). In general, making the comparison would require computing correlations functions in the strongly coupled CFT, but in a certain limit they can be found by a combination of conformal mappings and the method of images. In particular, the method of images is a useful way of imposing the correct ϕ periodicity, but is only justified if correlation functions satisfy free field equations so that solutions can be superimposed. This occurs when the string coupling in the bulk is taken to vanish, so in this limit we can check that the bulk and boundary correlators agree.

We proceed by applying an appropriate conformal transformation to the two point function on the infinite w -plane

$$\langle \mathcal{O}(w_+, w_-) \mathcal{O}(w'_+, w'_-) \rangle \sim \frac{1}{(\Delta w_+ \Delta w_-)^{2h_+}}. \quad (3.23)$$

For instance, consider a thermal expectation value corresponding to inserting both operators on the same boundary component. According to (3.18) we are to evaluate the two-point function on a torus with identifications $(u_+, u_-) \cong (u_+ + 2\pi, u_- + 2\pi) \cong (u_+ - i/T_+, u_- - i/T_-)$. By defining w_{\pm} as

$$w_{\pm} = e^{2\pi T_{\pm} u_{\pm}} \quad (3.24)$$

and including a sum over images under $w_{\pm} \rightarrow e^{(2\pi)^2 n T_{\pm}} w_{\pm}$ we account for the correct periodicities. Transforming the w -plane two-point function (3.23) (with the sum over images) to the u -frame we recover the result in (3.9). This is as it should be, since (3.24) is the asymptotic relation between Poincaré and BTZ coordinates; see (3.6). The same story holds for the other two-point functions except that we use a different conformal map for the two operators. It would be interesting to repeat this analysis in the case of nonvanishing string coupling.

3.2. Discussion

We have given rules for relating two-point functions in the bulk to two-point function in the CFT defined on the disconnected BTZ boundary. Analytic continuation allowed us to extend the bulk-boundary propagator from one region to the full geometry, and the two-point functions then follow in the usual fashion. The same procedure on the boundary side corresponds to considering various tensor product states depending on which boundaries operators are inserted. This procedure could clearly be extended to higher point correlators.

An important question is whether the analytic continuation is physically sensible. First, as we have stressed, this procedure implicitly chooses a particular state of the system (the Hartle-Hawking state) which may or may not be physically realizable. In particular, it is well known that the one-loop expectation value of the energy-momentum tensor of a free scalar field in this state suffers a divergence at the inner horizon [29]; this is a possible mechanism for excising the regions with closed timelike curves. So one can argue that any classical calculations sensitive to the geometry at the inner horizon are unreliable. Related issues have been discussed recently in the context of time dependent orbifolds of flat spacetime [30,31,32,32,33,34,35,36,37].

The physics at the inner horizon is unfortunately somewhat inaccessible with current string theory technology. The main problem is that direct calculations are only feasible

in the Euclidean signature target space, but the inner horizon is then absent. A priori, there are no obvious sources of divergences in one-loop Euclidean signature calculations that would continue over to divergences at the inner horizon. Indeed, note that Euclidean BTZ is equivalent to Euclidean “thermal AdS₃” [38], and the Lorentzian version of the latter is not expected to receive large quantum corrections. Obviously, these issues need to be much better understood, but since any more complete approach should eventually be compared with results based on the naive classical geometry it seems useful to develop those first, as we are doing here.

Another issue concerns the geometry of the boundary on which the dual CFT lives. In BTZ coordinates it is manifest that the boundary is conformal to a disconnected sum of cylinders, with spacelike and timelike circle directions in regions 1 and 3. The rules of AdS/CFT tell us that the CFT can be taken to live on this geometry. On the other hand since BTZ is an orbifold of AdS₃, and the latter has a connected cylindrical boundary, it was proposed in [13] that the CFT should live on this cylinder with twist operators inserted to account for the identifications. Note though that any connected boundary necessarily passes through region 2 behind the horizon, since it is not possible to go from region 1 to 3 without doing so. We do not wish to consider boundaries traversing the horizon, and so we prefer to work on the disconnected boundary at large radial BTZ coordinate.

4. SL(2,R) and SL(2,C)/SU(2) WZW models

We now turn to string theory. String theory on BTZ is described by an orbifold of the SL(2,R) WZW model. The spectrum of the SL(2,R) model was worked out in [6,39], and this was extended to the BTZ orbifold in [9] extending the work of [4]. Correlation functions of the SL(2,R) model were obtained in [22] by analytic continuation from the Euclidean signature SL(2,C)/SU(2) model, and we would now like the analogous story for BTZ. We begin by reviewing the salient aspects of the SL(2,R) and SL(2,C)/SU(2) WZW models.

4.1. Spectrum

The SL(2,R) WZW model is based on a $\widehat{SL}_k(2, R)_L \times \widehat{SL}_k(2, R)_R$ current algebra, Its Hilbert space therefore can be decomposed into various irreducible representations $\mathcal{D}_j^w, \mathcal{C}_{j,\alpha}^w$ of the current algebra,

$$\mathcal{H}_{AdS_3} = \bigoplus_{w=-\infty}^{\infty} \left[\left(\int_{\frac{1}{2}}^{\frac{k-1}{2}} dj \mathcal{D}_j^w \otimes \mathcal{D}_j^w \right) \oplus \left(\int_{\frac{1}{2}+iR} dj \int_0^1 d\alpha \mathcal{C}_{j,\alpha}^w \otimes \mathcal{C}_{j,\alpha}^w \right) \right] \quad (4.1)$$

where \mathcal{D}_j^w are the representations generated by spectral flow from the discrete representations \mathcal{D}_j^0 , and $\mathcal{C}_{j,\alpha}^w$ are the representations generated by spectral flow from the continuous

representations $\mathcal{C}_{j,\alpha}^0$, with an integer spectral flow parameter w . States in the former representations correspond to short strings in AdS_3 , while states in the latter representations correspond to long strings in AdS_3 .

The $\text{SL}(2,\mathbb{C})/\text{SU}(2)$ model has an $\widehat{SL}_k(2,C)$ current algebra, and its Hilbert space has the structure [23]

$$\mathcal{H}_{H_3} = \int_{s>0} ds s^2 \mathcal{D}_{\frac{1}{2}+is} \quad (4.2)$$

where \mathcal{D}_j are the principal series representations of the $\widehat{SL}_k(2,C)$ current algebra.

The connection between the $\text{SL}(2,\mathbb{R})$ and $\text{SL}(2,\mathbb{C})/\text{SU}(2)$ models is the following. In Poincaré coordinates with AdS_3 metric $ds^2 = d\phi^2 + e^{2\phi}d\gamma_+d\gamma_-$ the worldsheet action of the $\text{SL}(2,\mathbb{R})$ model is

$$\frac{k}{\pi} \int d^2z (\partial\phi\bar{\partial}\phi + e^{2\phi}\partial\gamma_-\bar{\partial}\gamma_+). \quad (4.3)$$

The analytic continuation to Euclidean signature H_3 corresponds to $\gamma_+ \rightarrow \gamma$, $\gamma_- \rightarrow \bar{\gamma}$, yielding the action

$$S = \frac{k}{\pi} \int d^2z (\partial\phi\bar{\partial}\phi + e^{2\phi}\bar{\partial}\gamma\partial\bar{\gamma}). \quad (4.4)$$

On the other hand, one can regard the coset $\text{SL}(2,\mathbb{C})/\text{SU}(2)$ as the space of matrices g parametrized by

$$g = \begin{pmatrix} e^{-\phi} + \gamma\bar{\gamma}e^{\phi} & e^{\phi}\gamma \\ e^{\phi}\bar{\gamma} & e^{\phi} \end{pmatrix}. \quad (4.5)$$

This follows from the fact that $g = hh^\dagger$ with $h \in \text{SL}(2,\mathbb{C})$. Then, substituting g into the standard form of the WZW action yields the action in (4.4).

The analytic continuation of the target space time coordinate creates subtleties when making connections with the two models. The first issue is associated with the normalizability of the associated string states. In the worldsheet theory, states in the Schrodinger picture are wavefunctionals $\Psi[x^\mu(\sigma)]$ where x^μ are the target space coordinates including the target space time coordinate t . Worldsheet normalizability is defined by integrating $|\Psi|^2$ over all $x^\mu(\sigma)$, so the target space time dependence enters into the normalizability condition.

From the worldsheet point of view all states in the Hilbert space of either theory are normalizable; note that we should allow for delta function normalizability due to the noncompact target space. We can choose a basis of states with time dependence $e^{-i\omega t}$, where t is the zero mode of the Lorentzian or Euclidean Poincaré time coordinate. Normalizability then requires boundary behavior $|\Phi| \sim e^{-p\phi}$, $p \geq 1$. Spin j primaries obey the wave equation for a minimally coupled scalar field

$$(\Delta - m^2) \Phi_j = 0, \quad m^2 = 4j(j-1), \quad (4.6)$$

where Δ is the Laplacian on $SL(2, \mathbb{R})$ or $SL(2, \mathbb{C})/SU(2)$. This equation has solutions with boundary behavior

$$\Phi_j \sim \begin{cases} e^{-2h_+\phi} & \text{Lorentzian} \\ e^{-2h_-\phi} & \text{Euclidean} \end{cases} \quad h_{\pm} = \frac{1}{2}(1 \pm \sqrt{1 + m^2}) . \quad (4.7)$$

In the Lorentzian case we can take any real m^2 and the h_+ branch, yielding normalizable primaries for any real j (but given the form of m^2 we can restrict to $j > \frac{1}{2}$) or $j = \frac{1}{2} + is$. In the Euclidean case we need $m^2 \leq -1$ or $j = \frac{1}{2} + is$. In the Lorentzian case with real j there is also the upper bound $j = (k - 1)/2$ which can be understood as the transition from short strings to long strings [6]. This accounts for the range of allowed j 's in (4.1) and (4.2).

What can be computed directly are correlation functions of the normalizable $j = \frac{1}{2} + is$ vertex operators in the $SL(2, \mathbb{C})/SU(2)$ model. The trouble is that in the AdS/CFT correspondence correlation functions in the boundary theory are related to correlation functions of non-normalizable vertex operators in the worldsheet CFT. These correspond to taking j real in the $SL(2, \mathbb{C})/SU(2)$ model, or j real and $h = h_-$ in the $SL(2, \mathbb{R})$ model. Such operators transform in nonunitary representations of $SL(2, \mathbb{C})$ and $SL(2, \mathbb{R})$. The strategy pursued in [22] was to start from the $j = \frac{1}{2} + is$ correlators of the $SL(2, \mathbb{C})/SU(2)$ model, and then analytically continue in j and the target space time coordinate in order to obtain correlation functions of non-normalizable vertex operators in the $SL(2, \mathbb{R})$ model. A sensible picture was obtained, with various singularities in the j -plane given physical interpretations. We follow a similar strategy, the difference being that we will focus on vertex operators consistent with the BTZ identifications, and we will analytically continue to the full extended Lorentzian BTZ geometry.

4.2. Vertex operators in the $SL(2, \mathbb{C})/SU(2)$ model

The primary operators of the model fall into the unitary irreducible representations of $SL(2, \mathbb{C})$, labelled by $j = \frac{1}{2} + is$ where s is a real number. In the semi-classical large k limit normal ordering issues can be neglected, and the primaries correspond to a complete set of normalizable solutions of (4.7)[23],

$$V_j(z, \bar{z}; x, \bar{x}) = \frac{1 - 2j}{\pi} ((\gamma - x)(\bar{\gamma} - \bar{x})e^{\phi} + e^{-\phi})^{-2j} . \quad (4.8)$$

The primaries are parameterized by the complex variable x ; (4.8) is just the usual bulk-boundary propagator in H_3 with x the coordinate on the boundary. More generally, the vertex operators must satisfy the correct operator product expansions with the $SL(2, \mathbb{C})$ currents,

$$\begin{aligned} J^a(z)V_j(z', \bar{z}'; x, \bar{x}) &\sim \frac{1}{z - z'} \mathcal{D}_j^a V_j(z', \bar{z}'; x, \bar{x}) \\ \bar{J}^a(\bar{z})V_j(z', \bar{z}'; x, \bar{x}) &\sim \frac{1}{\bar{z} - \bar{z}'} \bar{\mathcal{D}}_j^a V_j(z', \bar{z}'; x, \bar{x}) \end{aligned} \quad (4.9)$$

where $\mathcal{D}_j^a, \bar{\mathcal{D}}_j^a$ are the representation of the $\text{SL}(2, \mathbb{C})$ algebra generators, acting in the space of functions on C ,

$$\mathcal{D}_j^- = x^2 \frac{\partial}{\partial x} + 2jx, \quad \mathcal{D}_j^+ = \frac{\partial}{\partial x}, \quad \mathcal{D}_j^3 = x \frac{\partial}{\partial x} + j. \quad (4.10)$$

The operators are primaries with respect to the Virasoro algebra, with conformal weights Δ_j given by the Casimir $-j(j-1)$ of the representation,

$$\Delta_j = -\frac{j(j-1)}{k-2}. \quad (4.11)$$

The two-point functions for the vertex operators (4.8) were computed in [23] and found to have the form

$$\langle V_j(z_1, \bar{z}_1; x_1, \bar{x}_1) V_{j'}(z_2, \bar{z}_2; x_2, \bar{x}_2) \rangle = \frac{1}{|z_{12}|^{4\Delta_j}} \left[\delta^2(x_{12}) \delta(j+j'-1) + \frac{B(j)}{|x_{12}|^{4j}} \delta(j-j') \right] \quad (4.12)$$

where the coefficient $B(j)$ is

$$B(j) = \frac{k-2}{\pi} \frac{\nu^{1-2j}}{\gamma\left(\frac{2j-1}{k-2}\right)} \quad (4.13)$$

and

$$\gamma(x) \equiv \frac{\Gamma(x)}{\Gamma(1-x)}, \quad \nu \equiv \pi \frac{\Gamma(1 - \frac{1}{k-2})}{\Gamma(1 + \frac{1}{k-2})}. \quad (4.14)$$

Correlation functions on the worldsheet correspond to correlation functions on the boundary CFT by the relation [40]

$$\frac{\langle \prod_i \int d^2 z_i V_{j_i}(z_i, \bar{z}_i; x_i, \bar{x}_i) \rangle_{ws}}{\text{Vol}(\text{SL}(2, \mathbb{C}))} = \langle \prod_i V_{j_i}(x_i, \bar{x}_i) \rangle_{BCFT}. \quad (4.15)$$

For three-point or higher correlation functions one can cancel three of the $d^2 z$ integrals against $\text{Vol}(\text{SL}(2, \mathbb{C}))$ to get a finite result on the left hand side. But for the two-point function one is still left in the denominator with the volume of the $\text{SL}(2, \mathbb{C})$ subgroup leaving two points fixed (the dilatation group). The volume is infinite, but it can cancel the divergence coming from the delta function $\delta(j-j')$ [41]. In the process a j dependent factor can appear, but this can be fixed by relating the result to a three-point function using a Ward identity [22]. One thereby obtains

$$\langle V_j(x_1, \bar{x}_1) V_j(x_2, \bar{x}_2) \rangle_{BCFT} = \frac{(2j-1)B(j)}{|x_{12}|^{4j}}. \quad (4.16)$$

It is also useful to employ a momentum space basis for the primaries, using the transformation

$$V_j(z, \bar{z}; x, \bar{x}) = \sum_{m, \bar{m}} V_{j; m, \bar{m}}(z, \bar{z}) x^{m-j} \bar{x}^{\bar{m}-j} \quad (4.17)$$

and the inverse transformation

$$V_{j;m,\bar{m}}(z, \bar{z}) = \frac{1}{4\pi^2} \int d^2x |x|^{-2} x^{j-m} \bar{x}^{j-\bar{m}} V_j(z, \bar{z}; x, \bar{x}) . \quad (4.18)$$

One finds

$$\langle V_{j,m,j,\bar{m}} V_{j',m',j',\bar{m}'} \rangle_{\text{BCFT}} = \delta^2(m+m') \frac{\pi \Gamma(1-2j) \Gamma(j+m) \Gamma(j-\bar{m})}{\Gamma(2j) \Gamma(1-j+m) \Gamma(1-j-\bar{m})} (2j-1) B(j) . \quad (4.19)$$

(4.19) can now be interpreted as a two point function in Lorentzian AdS₃ by analytically continuing in j . The pole structure in the j -plane was given a physical interpretation in [22].

As stated, (4.19) gives the two-point function for $w = 0$ operators without spectral flow. Let us then consider two-point functions for spectral flowed states. Spectral flow acts on the current algebra generators and Virasoro operators as follows:

$$\begin{aligned} J_n^3 &= \tilde{J}_n^3 + \frac{k}{2} w \delta_{n,0} \\ J_n^\pm &= \tilde{J}_{n \mp w}^\pm \\ L_n &= \tilde{L}_n - w \tilde{J}_n^3 - \frac{k}{4} w^2 \delta_{n,0} . \end{aligned} \quad (4.20)$$

Following [22], we interpret the generators with tildes on top as those of the unflowed basis and without tildes as those of the spectral flowed basis; the notation for the eigenvalues is j, m, Δ_j in the unflowed basis and J, M, Δ_J in the flowed basis.

In [22], several spectral flowed two-point functions were discussed. The simplest case is when the vertex operators in the J, M basis create lowest or highest weight states $J = M$ in the representations d_J^\pm . A generic state in the unflowed representation d_j^\pm can always be mapped to such states by a suitable amount of spectral flow. Since one already knows the 2-point function (4.19) in the unflowed basis, one can then obtain the 2-point function for the $J = M$ states simply by replacing the labels:

$$m = M - \frac{k}{2} w, \quad \bar{m} = \bar{M} - \frac{k}{2} w . \quad (4.21)$$

Similarly, in the worldsheet 2-point function, one only needs to modify the powers of z, \bar{z} by replacing the correct conformal weights:

$$\Delta_j \rightarrow \Delta_J = \Delta_j - w m - \frac{k}{4} w^2, \quad \bar{\Delta}_j \rightarrow \bar{\Delta}_J = \bar{\Delta}_j - w \bar{m} - \frac{k}{4} w^2 . \quad (4.22)$$

The worldsheet two-point function ends up being [22]

$$\begin{aligned} &\langle V_{J,M,\bar{J},\bar{M}}(z_1, \bar{z}_1) V_{J',M',\bar{J}',\bar{M}'}(z_2, \bar{z}_2) \rangle \\ &= \frac{\delta^2(M+M')}{z_{12}^{2\Delta_J} \bar{z}_{12}^{2\bar{\Delta}_J}} \left(\delta(j+j'-1) + \delta(j-j') \frac{\pi B(j)}{\gamma(2j)} \frac{\Gamma(j+m) \Gamma(j-\bar{m})}{\Gamma(1-j+m) \Gamma(1-j-\bar{m})} \right) \end{aligned} \quad (4.23)$$

with the eigenvalues related by (4.21), (4.22). Specific choices for the spin j then give two-point functions for either spectral flowed short or long strings; the resulting expressions can be found in [22].

5. Two-point functions for strings in BTZ

Previously we discussed 2-point functions in BTZ in the supergravity approximation. Now we want to do the same in the full string theory. In other words, we will now generalize the results of [22], as reviewed in the previous section, to BTZ black holes. The starting point of the discussion in section 4 was the vertex operators (4.8) which transformed as tensors of conformal weight (j, j) on the boundary. Semi-classically, the vertex operators (4.8) were identified with the bulk-boundary propagator. As discussed in section 3, the BTZ bulk-boundary propagator is obtained by transforming the AdS₃ propagator and including a sum over images. Its asymptotic form with both arguments in region 1₊₊ is written in (3.7); it is extended to the other regions by analytic continuation. If we then replace the bulk coordinates r, u_{\pm} with the embedding of the string world sheet $r(z, \bar{z}), u_{\pm}(z, \bar{z})$, we can interpret the bulk-boundary propagator as the weight (j, j) string vertex operator labelled by u'_{\pm} ,

$$V_j(z, \bar{z}; u'_+, u'_-) = K_{\text{BTZ}}(r(z, \bar{z}), u_+(z, \bar{z}), u_-(z, \bar{z}); u'_+, u'_-) . \quad (5.1)$$

Being an orbifold of AdS₃, string theory on BTZ also has twisted sector vertex operators. These are included in the spectral flow operation, to be reviewed below.

5.1. String spectrum in BTZ

Let us now review some facts about the spectrum of strings in BTZ [4] [9]. To build the Hilbert space, we again start from the $\widehat{SL}_k(2, R)_L \times \widehat{SL}_k(2, R)_R$ current algebra. For AdS₃ it is convenient to work in the elliptic basis, which includes translation generators for the global coordinates τ and θ . For strings in BTZ black holes we instead want translation generators for BTZ t and ϕ . This is the hyperbolic basis and corresponds to diagonalizing the non-compact generators J_n^2, \bar{J}_n^2 . In the hyperbolic basis the current algebra commutation relations take the form

$$\begin{aligned} [J_n^2, J_m^{\pm}] &= \pm i J_{n+m}^{\pm} \\ [J_n^+, J_m^-] &= -2i J_{n+m}^2 - kn \delta_{n+m,0} \\ [J_n^2, J_m^2] &= \frac{k}{2} n \delta_{n+m,0} . \end{aligned} \quad (5.2)$$

Time translations and rotations in BTZ coordinates are generated by the following combinations of zero modes of J^2, \bar{J}^2 :

$$\begin{aligned} Q_t &= 2\pi T_+ J_0^2 - 2\pi T_- \bar{J}_0^2 \\ Q_\phi &= 2\pi T_+ J_0^2 + 2\pi T_- \bar{J}_0^2 \end{aligned} \quad (5.3)$$

(up to additional constant terms for winding modes, see [9]). The eigenvalues J_L, J_R of the non-compact global $\text{SL}(2, \mathbb{R})$ generators J_0^2, \bar{J}_0^2 have a continuous spectrum. That, along with the form of the commutation relations in the hyperbolic basis, make it slightly more complicated to recognize the standard discrete and continuous unitary irreps of the global $\text{SL}(2, \mathbb{R}) \times \text{SL}(2, \mathbb{R})$ algebra. For details, see [9,4]. After constructing the standard representations of the global algebra, one can proceed to construct the representations of the current algebra. The states in the representations have the form [4]

$$K_N |J_R, r\rangle \bar{K}_N |J_L, r\rangle \quad (5.4)$$

where K_N is a generic product of operators K_{-n}^a defined by

$$K_{-n}^2 \equiv J_{-n}^2, \quad K_{-n}^+ \equiv J_{-n}^+ J_0^-, \quad K_{-n}^- \equiv J_{-n}^- J_0^+ . \quad (5.5)$$

These satisfy the commutation rules

$$[J_0^2, K_{-n}^a] = 0, \quad [L_0, K_{-n}^\pm] = n K_{-n}^\pm . \quad (5.6)$$

Spectral flow in the hyperbolic basis generates strings which wind around the horizon of the BTZ black hole. The action on the group elements is

$$g \rightarrow e^{-iw_+ x^+ \tau^2} g e^{iw_- x^- \tau^2} . \quad (5.7)$$

In particular, the BTZ coordinates transform as

$$u_\pm(\sigma, \tau) \rightarrow u_\pm(\sigma, \tau) + \frac{w_\pm}{2\pi T_\pm} (\sigma \pm \tau) . \quad (5.8)$$

After the periodic identifications which make the BTZ black hole, the spectral flow parameters are constrained to discrete values

$$w_\pm = 2\pi T_\pm n , \quad (5.9)$$

so as to respect the periodicity of the worldsheet. Under spectral flow, the components of J^2, \bar{J}^2 transform as

$$\begin{aligned} J_n^2 &\rightarrow \tilde{J}_n^2 \equiv J_n^2 + \frac{k}{2} w_+ \delta_{n,0}, & J_n^\pm &\rightarrow \tilde{J}_n^\pm \equiv J_{n \pm iw_+}^\pm \\ \bar{J}_n^2 &\rightarrow \tilde{\bar{J}}_n^2 \equiv \bar{J}_n^2 - \frac{k}{2} w_- \delta_{n,0}, & \bar{J}_n^\pm &\rightarrow \tilde{\bar{J}}_n^\pm \equiv \bar{J}_{n \pm iw_-}^\pm \end{aligned} \quad (5.10)$$

and the Virasoro generators are found to transform as

$$\begin{aligned} L_n &\rightarrow L_n + w_+ J_n^2 + \frac{k}{4} w_+^2 \delta_{n,0} \\ \bar{L}_n &\rightarrow \bar{L}_n - w_- \bar{J}_n^2 + \frac{k}{4} w_-^2 \delta_{n,0} . \end{aligned} \tag{5.11}$$

The vertex operators for the Kac-Moody primaries, transforming under the unitary irreducible representations of the global algebra, have the form

$$V_{J_R, J_L}^{j,0} = D_{J_R, J_L}^j(g) e^{-iJ_R \hat{u} + iJ_L \hat{v}} , \tag{5.12}$$

where $\hat{u} = \pi T_+ u_+$, $\hat{v} = -\pi T_- u_-$. The vertex operators $V_{J_R, J_L}^{j,n}(z, \bar{z})$ in the twisted sector are constructed with the help of twist fields $W_n(z, \bar{z})$,

$$V_{J_R, J_L}^{j,n}(z, \bar{z}) = V_{J_R, J_L}^{j,0}(z, \bar{z}) W_n(z, \bar{z}) . \tag{5.13}$$

The Kac-Moody primaries are then the states

$$|j, J_R, n\rangle |j, J_L, n\rangle = V_{J_R, J_L}^{j,n} |0\rangle |0\rangle . \tag{5.14}$$

Alternatively, the twisted sector states can be interpreted as the spectral flowed states with integer flow parameter n .⁴

The target space energy spectrum for the string states is continuous, unlike in pure AdS₃ where the spectrum of short strings is discrete. The target space energy is given by the eigenvalue of the time translation generator Q_t , which involves continuous eigenvalues for the operators J_0^2, \bar{J}_0^2 . More discussion can be found in [9].

The preceding construction gives us the spectrum of strings located in, say, region 1_{++} outside the horizon. In what sense are the strings localized in a given region, and how do we obtain the string states in the other regions? We chose to diagonalize the zero mode generators in the hyperbolic basis; these act as isometry generators in a given coordinate patch of the BTZ spacetime. Therefore, the center of mass coordinates of the string are confined to a given patch. On the other hand, the full wavefunction of the string spreads out into the other regions. This becomes clear if one thinks of starting with a string state in AdS₃ and then imposing the BTZ identifications — the original state spreads out over the whole AdS₃ spacetime, and the identifications affect only the center of mass coordinates, thus the final state spreads out over the whole BTZ spacetime. Our spectrum therefore

⁴ In addition, there is one subtle part of the spectrum which was not discussed in [4,9], the discrete set of vacua [5]. These presumably correspond to the vacua defined with respect to each spectral flowed basis of the current algebra. We thank Y. Satoh for bringing this to our attention.

includes strings that straddle the horizon, a picture which is reminiscent of strings ending on a D-brane, and which has been suggested to be responsible for black hole entropy (for discussion, see e.g. [42]). The other issue concerns strings with center of mass coordinates in the different regions. Since the WZW model takes the same form in all regions, it is clear that the analysis is essentially identical in all cases. The only difference is that the coordinate range of r is different in region 2 from regions 1 and 3, but this just affects one's choice for a complete basis of solutions to the wave equation in a given region. So modulo this fact, we get the same spectrum of strings in all regions. Actually, in order for interactions to be well behaved the center of mass wavefunctions should continue smoothly from one region to a neighboring region. Exactly as in field theory, this can correlate positive and negative frequency wavefunctions in adjacent regions, and is responsible for Hawking radiation.

5.2. Identifying the vertex operators

In order to relate the vertex operators proposed in (5.1) with the Kac-Moody primaries (5.12), we need to first transform the former from the (j, u'_+, u'_-) basis to the (j, J_R, J_L) basis. Note first that the operators (5.1) included a sum over images which rendered them periodic in ϕ — they are of the form

$$V_j(z, \bar{z}; u'_+, u'_-) = \sum_{n=-\infty}^{\infty} \tilde{V}_j(z, \bar{z}; u'_+ + 2\pi n, u'_- + 2\pi n) , \quad (5.15)$$

where \tilde{V}_j is equal to (3.7) without the sum. We can express them as Fourier integrals (we simplify the notation and drop the primes from the boundary coordinates)

$$V_j(z, \bar{z}; u_+, u_-) = \sum_{k=-\infty}^{\infty} \int d\omega V_{j,\omega,k} e^{+i(\frac{\omega-k}{2})u_+ - i(\frac{\omega+k}{2})u_-} , \quad (5.16)$$

with the inverse transformation

$$V_{j,\omega,k} = \frac{1}{4\pi^2} \int du_+ \int du_- e^{-i(\frac{\omega-k}{2})u_+ + i(\frac{\omega+k}{2})u_-} V_j(z, \bar{z}; u_+, u_-) . \quad (5.17)$$

On the boundary, J_0^2, \bar{J}_0^2 are represented by

$$\begin{aligned} D^2 &= -i \frac{1}{2\pi T_+} \partial_{u_+} \\ \bar{D}^2 &= -i \frac{1}{2\pi T_-} \partial_{u_-} . \end{aligned} \quad (5.18)$$

The Fourier modes are their eigenfunctions with eigenvalues

$$J_R = \frac{\omega - k}{4\pi T_+}, \quad J_L = -\frac{\omega + k}{4\pi T_-} . \quad (5.19)$$

The J_R, J_L have continuous real eigenvalues as expected, and thus we can denote the vertex operators in Fourier space by V_{j, J_R, J_L} as in the previous section.

We will now move on to compute the 2-point functions for strings in BTZ. The calculations are based on those in [23] and [22], so we need to perform an analytic continuation to Euclidean BTZ geometry.

5.3. Euclidean section

As in Section 3, we are going to work in the Euclidean geometry. The Euclidean section for the BTZ black hole is obtained by

$$\begin{aligned} u_+ \rightarrow u = \phi + i\tau, \quad u_- \rightarrow \bar{u} = \phi - i\tau, \\ T_+ \rightarrow T, \quad T_- \rightarrow \bar{T}. \end{aligned} \tag{5.20}$$

The boundary of the Euclidean BTZ is a torus

$$u \sim u + 2\pi, \quad u \sim u + i\beta \tag{5.21}$$

where $\beta = 1/T = \beta_1 + i\beta_2$ is the complex inverse temperature. Now we need to Fourier expand the vertex operators $V_j(z, \bar{z}; u, \bar{u})$ with mode functions $f_{m, \bar{m}}$ which are periodic on the torus,

$$f_{m, \bar{m}}(\phi, \tau) = e^{i(m - \bar{m})\phi + \frac{i}{\beta_1}[(2\pi + \beta_2)m + (2\pi - \beta_2)\bar{m}]\tau}, \tag{5.22}$$

the expansion is

$$V_j(z, \bar{z}; u, \bar{u}) = \sum_{m, \bar{m}} V_{j, m, \bar{m}} f_{m, \bar{m}}(\phi, \tau) \tag{5.23}$$

and the inverse transformation is

$$V_{j, m, \bar{m}} = \int_0^{2\pi} d\phi \int_0^{\beta_1} \frac{d\tau}{\beta_1} f_{-m, -\bar{m}}(\phi, \tau) V_j(z, \bar{z}; u, \bar{u}). \tag{5.24}$$

The functions $f_{m, \bar{m}}$ are of course again eigenmodes of the generators J_0^2, \bar{J}_0^2 . On the Euclidean boundary, J_0^2, \bar{J}_0^2 are represented by

$$\begin{aligned} D^2 &= -i \frac{\beta}{2\pi} \partial_u \\ \bar{D}^2 &= -i \frac{\bar{\beta}}{2\pi} \partial_{\bar{u}}. \end{aligned} \tag{5.25}$$

The functions $f_{m, \bar{m}}$ satisfy

$$\begin{aligned} D^2 f_{m, \bar{m}}(u, \bar{u}) &= -\frac{i\beta}{4\pi\beta_1} [(2\pi + i\bar{\beta})m + (2\pi - i\bar{\beta})\bar{m}] f_{m, \bar{m}}(u, \bar{u}) \equiv +i\alpha f_{m, \bar{m}}(u, \bar{u}) \\ \bar{D}^2 f_{m, \bar{m}}(u, \bar{u}) &= \frac{i\bar{\beta}}{4\pi\beta_1} [(2\pi - i\beta)m + (2\pi + i\beta)\bar{m}] f_{m, \bar{m}}(u, \bar{u}) \equiv -i\bar{\alpha} f_{m, \bar{m}}(u, \bar{u}). \end{aligned} \tag{5.26}$$

Thus, in the Euclidean geometry the eigenvalues J_R, J_L take the values

$$\begin{aligned} J_R &= i\alpha = -\frac{i\beta}{4\pi\beta_1} [(2\pi + i\bar{\beta})m + (2\pi - i\bar{\beta})\bar{m}] \\ J_L &= -i\bar{\alpha} = \frac{i\bar{\beta}}{4\pi\beta_1} [(2\pi - i\beta)m + (2\pi + i\beta)\bar{m}] . \end{aligned} \quad (5.27)$$

Note that now the eigenvalues J_R, J_L take discrete complex values. This is a property of the Euclidean section, following from the double periodicity of the mode functions (5.22) on the Euclidean toroidal boundary. In analytically continuing back to the Lorentzian section, the mode functions (5.22) need to be continued to those in (5.16) which are only periodic in the angle coordinate. Therefore, in addition to continuing back to real time coordinate, we also need to continue the parameters so that the eigenvalues (5.27) again take the form (5.19). Also, we first analytically continue both arguments of the two-point function to the same boundary component. Two-point functions on distinct boundary components are then obtained by further analytic continuation. We comment on these issues further after we have computed the 2-point function.

5.4. Two-point functions

Let us now label the vertex operators as $V_{j,i\alpha,-i\bar{\alpha}}$, and compute their two-point functions, the analogue of (4.19). It turns out that we can simply use the earlier results discussed in Section 3, if we express the inverse Fourier transformation formula (5.24) in the coordinates

$$x = e^{\frac{2\pi}{\beta}u}, \quad \bar{x} = e^{\frac{2\pi}{\bar{\beta}}\bar{u}}, \quad (5.28)$$

remembering that V transforms like a tensor. It then takes a similar form to (4.18),

$$V_{j;m,\bar{m}}(z, \bar{z}) = \frac{1}{8\pi^2} \left(\frac{4\pi^2}{\beta\bar{\beta}} \right)^{j-1} \int d^2x |x|^{-2} x^{j+\alpha} \bar{x}^{j-\bar{\alpha}} V_j(z, \bar{z}; x, \bar{x}) . \quad (5.29)$$

Since in the x, \bar{x} space the 2-point function is the same as (4.16), the result now has the same form as (4.18), but with the replacement

$$m \mapsto -\alpha, \quad \bar{m} \mapsto \bar{\alpha} . \quad (5.30)$$

So we obtain

$$\langle V_{j,i\alpha',j,-i\bar{\alpha}'} V_{j,i\alpha,j,-i\bar{\alpha}} \rangle_{\text{BCFT}} = \delta^2(\alpha' + \alpha) \frac{\pi(2j-1)B(j)\Gamma(1-2j)\Gamma(j+\alpha)\Gamma(j+\bar{\alpha})}{\Gamma(2j)\Gamma(1-j+\alpha)\Gamma(1-j+\bar{\alpha})} . \quad (5.31)$$

Note that we only know the two-point function at a discrete set of points $\alpha, \bar{\alpha}$ given by (5.27). This is analogous to what happens in finite temperature quantum field theory.

Usually the thermal Green's functions are calculated in the imaginary time formalism, and they are found only at the discrete set of Matsubara frequencies. To understand the result (5.31) better, let us compare it with the two-point function previously obtained from a supergravity BTZ/CFT calculation [43]. Ref. [43] calculated the retarded CFT propagator in momentum space for a CFT operator which is dual to a supergravity field in the non-rotating BTZ black hole bulk geometry. The momentum space retarded propagator is defined by a Fourier transformation of the real time retarded propagator,

$$G_{ret}(\omega, k) = \int dt d\phi e^{-i\omega t + ik\phi} G_{ret}(t, \phi) \quad (5.32)$$

and the result [43] is

$$G_{ret}(\omega, k) = \frac{\Gamma(1 - \nu)\Gamma(h_+ - \frac{i}{2r_+}(\omega + k))\Gamma(h_+ - \frac{i}{2r_+}(\omega - k))}{\Gamma(1 + \nu)\Gamma(h_- - \frac{i}{2r_+}(\omega + k))\Gamma(h_- - \frac{i}{2r_+}(\omega - k))}, \quad (5.33)$$

where $h_+ = j$, $h_- = 1 - j$ and $1 + \nu = 2j$.⁵ Comparing the Fourier transformation formulas (5.19) and (5.24), we can establish the analytic continuation of the parameters

$$\alpha \leftrightarrow -\frac{i}{2r_+}(\omega - k), \quad \bar{\alpha} \leftrightarrow -\frac{i}{2r_+}(\omega + k). \quad (5.34)$$

With this relation, the propagator (5.31) has the same structure as (5.33). More precisely, the retarded CFT propagator (5.33) is a Fourier transform finite temperature propagator in real time. Hence it is known at a continuous set of frequencies ω . It is known that if we analytically continue it to the complex ω plane, and evaluate it at the discrete set of Matsubara frequencies, it is equal to the finite temperature thermal propagator calculated in the imaginary time formalism. For a brief review, see e.g. the Appendix of [44]. This is what happens here too. From (5.34), the frequencies are

$$\omega_n = ir_+(\alpha + \bar{\alpha}) = -ir_+(m + \bar{m}) \equiv -i2\pi n T_H, \quad (5.35)$$

which are just the expected Matsubara frequencies.⁶ Note also that

$$k = -ir_+(\alpha - \bar{\alpha}) = -m + \bar{m} = \text{integer}. \quad (5.36)$$

Consider then the pole structure of (5.31). There are two types of poles in the j -plane. First, there are poles arising from the $\Gamma(j - \alpha)\Gamma(j - \bar{\alpha})$ factors. These have a particle-like interpretation as a finite temperature effect due to the thermal density matrix

⁵ Note: eqn. (16) in [43] has a typo, R should be $\frac{R^2}{2r_+}$, we use $\ell = R$ and set $\ell = 1$.

⁶ We denote $n = m + \bar{m}$.

of the boundary theory. Second, there are poles arising from the factor $B(j)$. In [22] these were interpreted as worldsheet instantons arising from a holomorphic map of the spherical worldsheet onto the spherical boundary of Euclidean AdS_3 . Euclidean BTZ has a toroidal boundary, so at first sight one might be puzzled by the absence of a holomorphic map from a sphere to a torus. But recalling that the torus arises from the periodic identifications, we still have the worldsheet instantons but now they wrap the boundary torus multiple times.

In section 3 we discussed BCFT correlation functions on the extended boundary. It is straightforward to extend this discussion to string theory. We need to again transform from the J_R, J_L basis to the u_+, u_- -basis. First, the vertex operators (5.1) can be analytically continued to any of the other regions $1\eta_1\eta_2, 3\eta_1\eta_2$ by a suitable analytic continuation of the boundary coordinates u'_+, u'_- . In order to compute a BCFT 2-point function associated with a pair of such string states, it is convenient to start from the expression (4.16), use the transformation (5.28) and remember that the operators scale like (j, j) -tensors. In this way, one obtains for example the BCFT two-point function

$$\begin{aligned} & \langle V_j^{1++}(u_{+1}, u_{-1}) V_j^{1++}(u_{+2}, u_{-2}) \rangle_{\text{BCFT}} \\ &= \sum_{n=-\infty}^{\infty} \frac{(2j-1)B(j)}{[\sinh \pi T(\Delta u_+ + 2\pi n)]^{2j} [\sinh \pi T(\Delta u_- + 2\pi n)]^{2j}} \end{aligned} \quad (5.37)$$

Continuation to other regions is the same as in (3.9) (3.10).

5.5. Spectral flowed 2-point functions

Having obtained the two-point function for unflowed operators, we proceed as in Section 4 and compute the spectral flowed two-point function. For convenience, we first alter some of our notations somewhat. Let us denote the eigenvalues of J_0^2, \bar{J}_0^2 in the unflowed basis as J_R, J_L and in a flowed basis as $\mathbf{J}_R, \mathbf{J}_L$. We first write the worldsheet two-point function, and use the labels J_R, J_L instead of $\alpha, \bar{\alpha}$:

$$\begin{aligned} & \langle V_{j, J'_R, j, J'_L}(z_1, \bar{z}_1) V_{j, J_R, j, J_L}(z_2, \bar{z}_2) \rangle = |z_{12}|^{-4\Delta_j} \delta^2(J'_R + J_R) \times \\ & \left(\delta(j + j' - 1) + \delta(j - j') \frac{\pi(2j-1)B(j)\Gamma(1-2j)\Gamma(j-iJ_R)\Gamma(j+iJ_L)}{\Gamma(2j)\Gamma(1-j-iJ_R)\Gamma(1-j+iJ_L)} \right). \end{aligned} \quad (5.38)$$

Under spectral flow, this becomes

$$\begin{aligned} & \langle V_{j, \mathbf{J}'_R, j, \mathbf{J}'_L}(z_1, \bar{z}_1) V_{j, \mathbf{J}_R, j, \mathbf{J}_L}(z_2, \bar{z}_2) \rangle = z_{12}^{-2\Delta_j} \bar{z}_{12}^{-2\bar{\Delta}_j} \delta^2(J'_R + J_R) \times \\ & \left(\delta(j + j' - 1) + \delta(j - j') \frac{\pi(2j-1)B(j)\Gamma(1-2j)\Gamma(j-iJ_R)\Gamma(j+iJ_L)}{\Gamma(2j)\Gamma(1-j-iJ_R)\Gamma(1-j+iJ_L)} \right). \end{aligned} \quad (5.39)$$

with

$$J_R = \mathbf{J}_R + k\pi T n, \quad J_L = \mathbf{J}_L - k\pi \bar{T} n \quad (5.40)$$

and

$$\begin{aligned}\Delta_J &= \Delta_j - 2\pi T n \mathbf{J}_R - k(\pi T n)^2 \\ \bar{\Delta}_J &= \Delta_j + 2\pi \bar{T} n \mathbf{J}_L - k(\pi \bar{T} n)^2 .\end{aligned}\tag{5.41}$$

Note again that in the Euclidean section the parameters are complex valued. Therefore, the conformal weights $\Delta_J, \bar{\Delta}_J$ appear to be complex. However, we are interested in the 2-point functions in the Lorentzian section, so we must again remember to analytically continue all the parameters. Upon the analytic continuation, the parameters are replaced by their values in the Lorentzian BTZ geometry, which all take real values. In particular, the conformal weights are again real.

As before, specific choices for the spin j yield 2-point functions for short or long strings. In particular we can obtain two-point functions for strings which wind around the black hole.

6. Discussion

In this work we have discussed the computation of supergravity and string theory correlation functions in the background of the extended BTZ black hole. These were related to correlation functions in the dual CFT living on the disconnected boundary of the spacetime. The organizing principle was to use an appropriate analytic continuation from Euclidean signature. We conclude this paper with a discussion of some open questions related to our work.

- The main outstanding issue is probably that of backreaction. There are good reasons to expect large effects in the extended geometry due to the presence of closed timelike curves, and these could invalidate perturbation theory. This was pointed out in the original work [1], and related issues have been the subject of recent discussion [34,35,36,37]. In principle, this issue can be addressed by studying scattering processes. If perturbation theory is indeed breaking down, one can still hope to make some progress due to the fact that there is a well-defined holographic dual theory living on the boundary.
- The correlation functions that we have discussed are those of non-normalizable vertex operators, corresponding to inserting operators in the boundary CFT. These are the correlation functions which can be deduced by analytic continuation from Euclidean signature. On the other hand, in Lorentzian signature there are also normalizable vertex operators, and in fact it is these that transform in unitary representations of $SL(2,\mathbb{R}) \times SL(2,\mathbb{R})$. Experiments performed by physical observers correspond to transition amplitudes between normalizable states in the Hilbert space, and so in string theory should correspond to correlation functions of normalizable vertex operators. The normalizable correlation functions are in principle determined by the

non-normalizable ones, in the same way as in field theory the transition amplitudes between normalizable states are determined by the vacuum correlation functions, but this is somewhat indirect. On the other hand, computing these directly apparently requires working in Lorentzian signature, and dealing with the unboundedness of the corresponding worldsheet theory.

- One of the main motivations to study black hole spacetimes in string theory is to address the information paradox. To formulate the paradox one really needs to consider a situation in which a black hole forms from collapse and then evaporates completely (or conceivably leaves a remnant), since it is in this setup that unitarity and locality seem to clash. In the eternal black hole there is no paradox: information thrown at the black hole by one asymptotic observer may or may not be radiated back to this observer; but if not, unitarity is retained simply by taking into account the other regions into which the information can flow. Studying the collapse scenario in string theory requires some new ingredients. In order to use worldsheet methods one needs a conformal field theory representing matter collapsing to form a black hole. This is clearly a situation in which continuation to Euclidean signature is impossible, so one has to learn to compute in Lorentzian signature. Hopefully, the lessons learned from studying toy models like time-dependent orbifolds will be of use here.

Acknowledgements: We thank Danny Birmingham and Ivo Sachs for discussions, and Stephen Hwang and Yuji Satoh for additional correspondence. S.H. was supported in part by the Magnus Ehrnrooth Foundation, E.K-V. was supported in part by the Academy of Finland, and P.K. was supported by NSF grant PHY-0099590. E.K-V. would also like to thank the University of California at Los Angeles and Institute for Theoretical Physics in Amsterdam for hospitality while this work was in progress.

References

- [1] M. Banados, C. Teitelboim and J. Zanelli, Phys. Rev. Lett. **69**, 1849 (1992) [arXiv:hep-th/9204099]; M. Banados, M. Henneaux, C. Teitelboim and J. Zanelli, Phys. Rev. D **48**, 1506 (1993) [arXiv:gr-qc/9302012].
- [2] G. T. Horowitz and D. L. Welch, Phys. Rev. Lett. **71**, 328 (1993) [arXiv:hep-th/9302126].
- [3] N. Kaloper, Phys. Rev. D **48**, 2598 (1993) [arXiv:hep-th/9303007].
- [4] M. Natsuume and Y. Satoh, Int. J. Mod. Phys. A **13**, 1229 (1998) [arXiv:hep-th/9611041].
- [5] Y. Satoh, Nucl. Phys. B **513**, 213 (1998) [arXiv:hep-th/9705208].
- [6] J. M. Maldacena and H. Ooguri, J. Math. Phys. **42**, 2929 (2001) [arXiv:hep-th/0001053].
- [7] M. Henningson, S. Hwang, P. Roberts and B. Sundborg, Phys. Lett. B **267**, 350 (1991).
- [8] S. Hwang and P. Roberts, arXiv:hep-th/9211075.
- [9] S. Hemming and E. Keski-Vakkuri, Nucl. Phys. B **626**, 363 (2002) [arXiv:hep-th/0110252].
- [10] A. Giveon, D. Kutasov and N. Seiberg, Adv. Theor. Math. Phys. **2**, 733 (1998) [arXiv:hep-th/9806194].
- [11] E. J. Martinec and W. McElgin, JHEP **0204**, 029 (2002) [arXiv:hep-th/0106171].
- [12] J. Son, arXiv:hep-th/0107131.
- [13] E. J. Martinec and W. McElgin, arXiv:hep-th/0206175.
- [14] J. Troost, arXiv:hep-th/0206118.
- [15] S. Elitzur, A. Giveon, D. Kutasov and E. Rabinovici, JHEP **0206**, 017 (2002) [arXiv:hep-th/0204189].
- [16] B. Craps, D. Kutasov and G. Rajesh, JHEP **0206**, 053 (2002) [arXiv:hep-th/0205101].
- [17] L. Cornalba, M. S. Costa and C. Kounnas, arXiv:hep-th/0204261.
- [18] G. T. Horowitz and D. Marolf, JHEP **9807**, 014 (1998) [arXiv:hep-th/9805207].
- [19] V. Balasubramanian, P. Kraus, A. E. Lawrence and S. P. Trivedi, Phys. Rev. D **59**, 104021 (1999) [arXiv:hep-th/9808017].
- [20] B. G. Carneiro da Cunha, Phys. Rev. D **65**, 104025 (2002) [arXiv:hep-th/0110169].
- [21] J. M. Maldacena, arXiv:hep-th/0106112.
- [22] J. M. Maldacena and H. Ooguri, Phys. Rev. D **65**, 106006 (2002) [arXiv:hep-th/0111180].
- [23] J. Teschner, Nucl. Phys. B **546**, 390 (1999) [arXiv:hep-th/9712256]; Nucl. Phys. B **571**, 555 (2000) [arXiv:hep-th/9906215].
- [24] V. Balasubramanian and P. Kraus, Commun. Math. Phys. **208**, 413 (1999) [arXiv:hep-th/9902121].

- [25] S. S. Gubser, I. R. Klebanov and A. M. Polyakov, Phys. Lett. B **428**, 105 (1998) [arXiv:hep-th/9802109].
- [26] E. Witten, Adv. Theor. Math. Phys. **2**, 253 (1998) [arXiv:hep-th/9802150].
- [27] E. Keski-Vakkuri, Phys. Rev. D **59**, 104001 (1999) [arXiv:hep-th/9808037].
- [28] V. Balasubramanian, P. Kraus and A. E. Lawrence, Phys. Rev. D **59**, 046003 (1999) [arXiv:hep-th/9805171].
- [29] G. Lifschytz and M. Ortiz, Phys. Rev. D **49**, 1929 (1994) [arXiv:gr-qc/9310008].
- [30] V. Balasubramanian, S. F. Hassan, E. Keski-Vakkuri and A. Naqvi, arXiv:hep-th/0202187.
- [31] L. Cornalba and M. S. Costa, arXiv:hep-th/0203031.
- [32] N. A. Nekrasov, arXiv:hep-th/0203112.
- [33] J. Simon, JHEP **0206**, 001 (2002) [arXiv:hep-th/0203201].
- [34] H. Liu, G. Moore and N. Seiberg, JHEP **0206**, 045 (2002) [arXiv:hep-th/0204168]; arXiv:hep-th/0206182.
- [35] A. Lawrence, arXiv:hep-th/0205288.
- [36] M. Fabinger and J. McGreevy, arXiv:hep-th/0206196.
- [37] G. T. Horowitz and J. Polchinski, arXiv:hep-th/0206228.
- [38] J. M. Maldacena and A. Strominger, JHEP **9812**, 005 (1998) [arXiv:hep-th/9804085].
- [39] J. M. Maldacena, H. Ooguri and J. Son, J. Math. Phys. **42**, 2961 (2001) [arXiv:hep-th/0005183].
- [40] J. de Boer, H. Ooguri, H. Robins and J. Tannenhauser, JHEP **9812**, 026 (1998) [arXiv:hep-th/9812046].
- [41] D. Kutasov and N. Seiberg, JHEP **9904**, 008 (1999) [arXiv:hep-th/9903219].
- [42] L. Susskind and J. Uglum, Nucl. Phys. Proc. Suppl. **45BC**, 115 (1996) [arXiv:hep-th/9511227].
- [43] U. H. Danielsson, E. Keski-Vakkuri and M. Kruczenski, Nucl. Phys. B **563**, 279 (1999) [arXiv:hep-th/9905227].
- [44] T. S. Evans, A. Gomez Nicola, R. J. Rivers and D. A. Steer, arXiv:hep-th/0204166.